PCCP

Accepted Manuscript

ROYAL SOCIETY OF CHEMISTRY

www.rsc.org/pccp

Journal Name

ARTICLE

Energy levels in $CaWO_4$:Tb^{3+}at high pressure

S. Mahlik[a,*], E. Cavalli[b], M. Amer[c], P. Boutinaud[d,*]

Received 00th January 20xx,
Accepted 00th January 20xx

DOI: 10.1039/x0xx00000x

www.rsc.org/

The luminescence properties of Tb^{3+} in $CaWO_4$ crystals are investigated under hydrostatic pressure up to 200 kbar, i. e. across the scheelite-to-fergusonite phase transition. It is shown that the typical blue ($^5D_3$) and green ($^5D_4$) emissions in this material are progressively quenched at room temperature as pressure is increased. This quenching is caused by a downshift of the charge transfer (or impurity trapped exciton) state that is formed between Tb^{3+} and nearby W^{6+} cations in conjunction with a pressure-induced increase of the lattice relaxation experienced by this excited state. An empirical model is introduced to calculate the evolution of the (Tb^{3+}-W^{6+}) charge transfer energy with pressure. Combined with the pressure dependence of the energy bandgap in $CaWO_4$, the model allows locating the 4f levels of Tb^{3+} relative to the fundamental host lattice for any pressure in the range 0-200 kbar.

1. Introduction

$CaWO_4$ is a classical phosphor that has been investigated for more than half a century[1]. It shows an efficient intrinsic blue luminescence upon UV or X-ray excitation[2-8]. It belongs to the scheelite family (space group $I4_1/a$, Z = 4), and its crystal structure consists of isolated (WO_4) tetrahedral units that are loosely bridged by (CaO_8) distorted dodecahedra. These units are responsible for the main absorption and emission properties. The lowest-lying excited levels are located in the UV region at about 265 nm (37735 cm^{-1})[3]. The absorption transition to these states is referred to as the host fundamental excitation (HFE) and is related to transitions from the valence band, essentially formed by 2p orbitals of oxygen, to the conduction band essentially formed by 5d orbitals of tungsten. These transitions are commonly ascribed to the spin and electric dipole allowed $^1A_1 \rightarrow {}^1T_2$ transition.[5] Emission follows internal relaxation to the $^3T_2$ state and subsequent $^3T_2 \rightarrow {}^1A_1$ charge transfer transition, partially allowed in consequence of the spin-orbit and electron-phonon couplings and can be interpreted as self-trapped excitons.[5]

The luminescence intensity is temperature independent up to 200 K. In the temperature region 200 - 300 K, energy migration and radiationless processes within the tungstate groups start to compete with radiative decay and both the intensity and the emission decay time significantly decrease. The room temperature decay time is close to 9 µs and the corresponding decay profile is single exponential[9,10].

A great amount of work has already been dedicated to the luminescence properties of trivalent rare-earth (RE) ions in $CaWO_4$. The RE^{3+} emission can be conveniently obtained through host sensitization, even if the presence of the blue tungstate luminescence overlapping the RE lines in the UV-excited emission spectra indicates that the efficiency of this process is in general rather limited[11-15].

In the case of Pr^{3+} or Tb^{3+} doped samples, the emission dynamics are influenced by the formation of an intermediate charge transfer state (or impurity trapped exciton state) that interferes with the 4f excited states of the dopants by creating new relaxation channels that lead to the quenching of otherwise emitting levels[14-28].

The ionization transition creates the Ln^{4+} ion (Ln = Tb, Pr) and an electron in the conduction band (e_{cb}). After ionization, the Coulomb attraction between Ln^{4+} and e_{cb} allows the system to exist in the bound state, which defines an impurity trapped exciton (ITE) state (also referred to praseodymium/terbium trapped exciton (PTE/TTE) state) in the past literature[17-27]. In the equivalent description of this process the excitation bands corresponding to Pr^{3+} (or Tb^{3+}) - W^{6+} intervalence charge transfer (IVCT) is considered as a transition where the electron is transferred from Pr^{3+} to nearby W^{6+} cations[15,29-35]. It should be noted that the different labels IVCT and ITE (or PTE/TTE) refer to the same phenomenon. In the case of $CaWO_4$ (because the conduction band is mainly formed by 5d orbitals of tungsten) we consider IVCT (or ITE) as the system consisting of a hole captured at Ln^{3+} (forming Ln^{4+}) and an electron localized at the neighbouring WO_4^{2-} group(s). These processes will be designed as CT (charge transfer) processes in the following.

The action of pressure on the structural and optical properties of $CaWO_4$, either undoped or doped with RE ions like Tb^{3+}, Pr^{3+} or Eu^{3+}, has also received attention. $CaWO_4$ presents a phase transition

[a] Institute of Experimental Physics, University of Gdańsk, WitaStwosza 57, 80-952 Gdańsk, Poland
[b] Dipartimento di Chimica Generale ed Inorganica, Chimica Analitica, Chimica Fisica, Università di Parma, Parma, Italy
[c] Clermont Université, UBP, Institut de Chimie de Clermont-Ferrand,BP 10448, F-63000 Clermont-Ferrand
[d] Clermont Université, ENSCCF, Institut de Chimie de Clermont-Ferrand,BP 10448, F-63000 Clermont-Ferrand.

* Corresponding author E-mails:philippe.boutinaud@ensccf.fr (P. B.) and s.mahlik@ug.edu.pl (S. M.)

from the tetragonal scheelite structure to the monoclinic fergusonite structure at pressures exceeding 100 kbar[36,37]. To our best knowledge, the optical properties of $CaWO_4$ have only been investigated in the range 0 - 100 kbar, i. e. below the phase transition. The pressure behavior of the luminescence has evidenced: (1) no significant shift of the emission maximum with pressure, unlike $CdWO_4$ and $MgWO_4$ wolframites, (2) continuous increase of the emission intensity with pressure, (3) slight decrease of the emission decay time, from 9 to 5 µs, in the range 0 - 100 kbar. The decay curves were found to be single exponential for all pressures[38]. Applying pressure on $CaWO_4:Tb^{3+}$ and $CaWO_4:Pr^{3+}$ induces in both cases a downshift of the CT state relative to the Pr^{3+} (or Tb^{3+}) 4f states. The result is a quenching of the $^3P_0$ (at 105 kbar) and $^1D_2$ (at 315 kbar) emissions in $CaWO_4:Pr^{3+}$ and of the $^5D_3$ (at 70 kbar) and $^5D_4$ (at 190 kbar) emissions in $CaWO_4:Tb^{3+}$. The pressure-induced downshift of the CT state is estimated at -17.4 cm^{-1}/kbar with and additional downshift of 3200 cm^{-1} across the tetragonal-to-monoclinic phase transition[14,18].

In this paper, we investigate the action of hydrostatic pressure on the energy levels structure of $CaWO_4:Tb^{3+}$. A model will also be proposed to account for the pressure-dependence of the CT energy.

2. Experimental

$CaWO_4$ crystals nominally doped with 0.5 mol% Tb^{3+} were grown by the flux growth method in the 1350-600 °C temperature range, using Na_2WO_4 as a solvent [15]. Analytical grade CaO (98%, Carlo Erba), Na_2CO_3 (99%, Aldrich), WO_3 (99%, Aldrich) and Tb_4O_7 (99.9%, Aldrich) were used as starting materials. The Tb^{3+} ions enter the Ca^{2+} sites with eightfold oxygen coordination (hereafter denoted at $Ca^{2+}(Tb^{3+})$ sites). The difference in charge is compensated by the accommodation of Na^+ ions present in the growth mixture or by the formation of cationic vacancies. The excitation source for collecting the time resolved spectra and luminescence decays consists of a PL 2143 A/SS laser pumping a PG 401/SH parametric optical generator that generates 30 ps pulses of tuned wavelength with frequency 10 Hz. The luminescence signals were detected using 2501S (Bruker Optics) spectrograph and a Hamamatsu C4334- 01 Streak Camera. The time resolved luminescence spectra were obtained by integration of the streak camera pictures over the time intervals, whereas luminescence decays were obtained by integration of the streak camera pictures over the wavelength intervals[39]. The experiments at high pressures were carried out using a Merrill-Bassett type diamond anvil cell (DAC)[40]. Poly (dimethylsiloxane) oil was used as the pressure-transmitting medium, and a ruby crystal was used as the pressure detector. All the measurements were carried out at room temperature.

3. Results and discussion

We know from previous reports that the Tb^{3+} emission in $CaWO_4:Tb^{3+}$ can be excited in the UV range below 320 nm, i. e. in correspondence of the host absorption (transitions from valence to

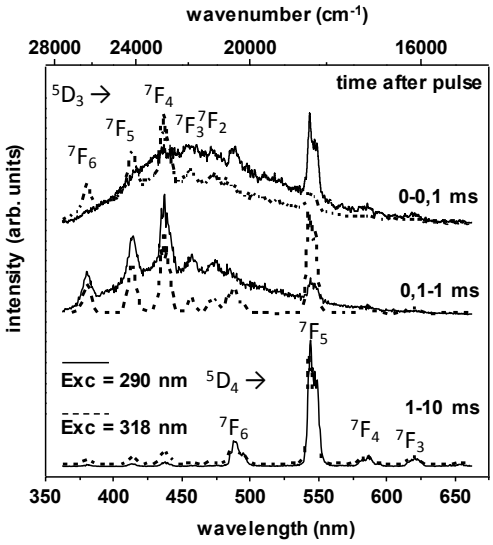

Fig. 1 Time-resolved emission spectra of $CaWO_4:Tb^{3+}$.

conduction band) and of ionization processes involving Tb^{3+} ions (transfer of an electron from Tb^{3+} ion to the bottom of the conduction band) considered as Tb^{3+} (4f) → W^{6+} (5d) CT transitions[15,18]. We show in Fig. 1 the time-resolved emission spectra of $CaWO_4:Tb^{3+}$ that were measured in the 0 - 10 ms range, at ambient pressure, upon pulsed excitation at 290 nm (host absorption) or 318 nm (internal 4f ($^7F_6$) → 4f ($^5H_6$) transition). The sharp lines observed in the 350 nm – 500 nm and 470 nm – 650 nm spectral ranges correspond to emissions from the $^5D_3$ and $^5D_4$ levels, respectively. The change in the relative intensity of the $^5D_3$ and $^5D_4$ emission lines with time has been addressed in details in Ref 15.

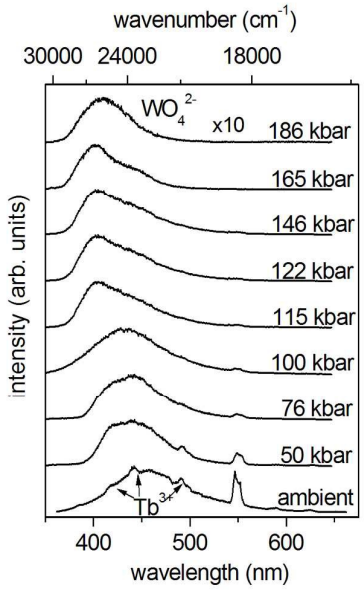

Fig. 2 Pressure dependence of the emission spectra of $CaWO_4:Tb^{3+}$.

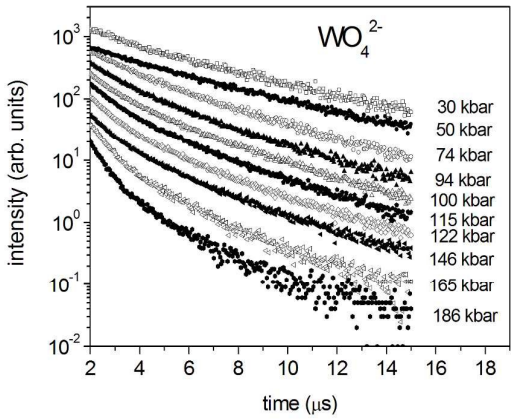

Fig. 3 Pressure dependence of the WO_4^{2-} emission in $CaWO_4:Tb^{3+}$.

Upon direct excitation in the Tb^{3+} levels, the $^5D_3$ lines dominate at short time but become weak at longer time, at the benefit of the $^5D_4$ lines. This behavior is the consequence a cross-relaxation effect[15]. Upon excitation in the conduction band states, the weakness of $^5D_3$ lines and the high intensity of the $^5D_4$ lines at short time are explained by the depopulation of the $^5D_3$ level through an intermediate CT state, resulting in the feeding of the $^5D_4$ level[15]. At short time, the Tb^{3+} lines overlap the broad WO_4^{2-} emission band that extends from 350 nm to 600 nm. The presence of this fast decaying band indicates that the WO_4^{2-}-Tb^{3+} energy transfer is not complete at ambient pressure. We show in Fig. 2 the time resolved emission spectra obtained at different pressures upon excitation at 290 nm. The time scale is reduced to 0 - 20 μs to magnify the host luminescence relative to the Tb^{3+} lines. The application of pressure (P) induces a blue shift of the band maximum and an increase of the intensity ratio between the WO_4^{2-} and Tb^{3+}-related features. We further note a significant alteration of the band shape in correspondence of the tetragonal-to-monoclinic phase transition (P > 100 kbar). Figs. 3 and 4 show the action of pressure on the decay profiles of the WO_4^{2-} and Tb^{3+} ($^5D_4$) emissions, respectively. In both cases, a complex evolution with pressure is observed. Average values of the time constant were determined using:

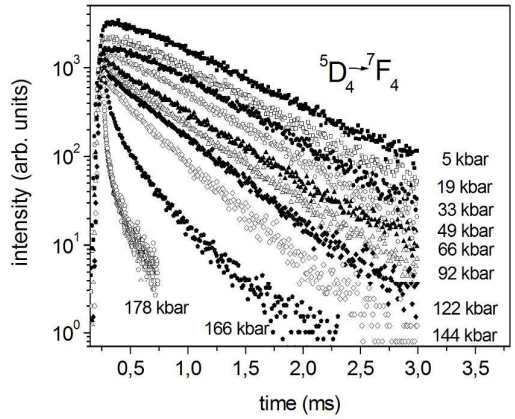

Fig. 4 Pressure dependence of the $^5D_4$ (Tb^{3+}) emission in $CaWO_4:Tb^{3+}$. Excitation at 290 nm.

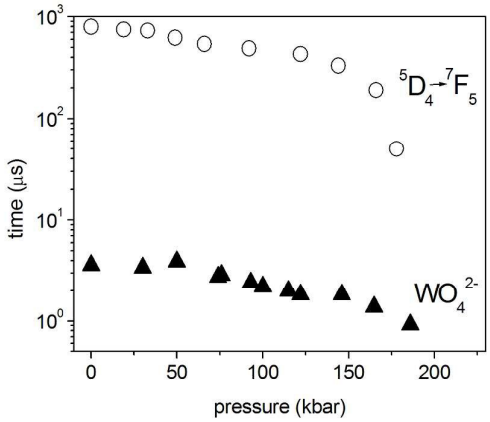

Fig. 5 Pressure dependence of the average time constants of WO_4^{2-} and $^5D_4$ (Tb^{3+}) emissions in $CaWO_4:Tb^{3+}$. Excitation at 290 nm.

$$\tau = \frac{\int t \cdot I(t)dt}{\int I(t)dt} \quad (1)$$

where *I(t)* represents the emission intensity at time t. The obtained values are plotted against pressure in Fig. 5.

Concerning the decay of the host crystal, it is known from previous reports that the decay time of $CaWO_4$ at room temperature and ambient pressure is only 9 μs[38], being the emission of this unit significantly affected by non-radiative losses ascribed to energy migration and internal thermal quenching[41]. In $CaWO_4:Tb^{3+}$, the decay time of the host becomes 4.5 μs in consequence of the host to Tb^{3+} energy transfer process, whose efficiency, η_{ET}, estimated using the equation:

$$\eta_{ET} = 1 - \frac{\tau_{doped}}{\tau_{undoped}} \quad (2)$$

is about 50 %. As described in Ref. 38, the application of pressure modifies the energy level diagram of the WO_4^{2-} unit, alters its probabilities of radiative and non-radiative decays, and finally its emission time-constant.

Other effects, like the pressure-induced modification of the structural parameters (especially the shrinkage of WO_4^{2-}-WO_4^{2-} and WO_4^{2-}-Ca^{2+}(Tb^{3+}) distances, see Fig. 6) should increase the efficiency of the WO_4^{2-}-Tb^{3+} energy transfer and shorten the decay times accordingly. The concomitancy of different processes accounts for the non-linear behavior of the WO_4^{2-} decay profiles upon application of pressure.

The Tb^{3+} decays also show complex evolution, especially across the phase transition. For the low pressures, the $^5D_4$ level is fed either from the $^5D_3$ level, by mean of cross-relaxation, or directly from the CT state. Upon applying pressure, the CT state undergoes an energy downshift that causes the progressive quenching of $^5D_4$ emission lines, which is clearly evidenced in Fig. 5 by the shortening of the corresponding emission time constant.

A few years ago[34,35], an empirical equation has been introduced to estimate the energy of the charge transfer state that is formed between Tb^{3+} and a transition metal (M^{n+}) with d^0 electron configuration. At ambient pressure (P=0), this equation has the form:

$$(Tb^{3+} - M^{n+}, cm^{-1})_0 = 58800 - 49800\,\frac{\chi_{opt}(M^{n+})}{d_0(Tb^{3+} - M^{n+})} \qquad (3)$$

Where $X_{opt}(M^{n+})$ is the optical electronegativity of the transition metal ion and $d_0(Tb^{3+}\text{-}M^{n+})$ is the shortest distance separating the cations at ambient pressure[34,35]. This distance corresponds to the $Ca^{2+}(Tb^{3+})$-W^{6+} distance in the lattice. Taking $X_{opt}(W^{6+})=2$[42] and a $Ca^{2+}(Tb^{3+})$-W^{6+} distance of 3.70 Å at ambient pressure, we calculate a CT energy of 31880 cm^{-1} (≈ 313 nm). This locates the corresponding CT band in correspondence of the edge of the excitation spectrum[15]. As stated above, the (Tb^{3+}-M^{n+}) CT is interpreted as an electronic transition from the $^7F_6$ ground state of Tb^{3+} to the bottom of the conduction band of the host lattice[43], mostly consisting of empty d states of M^{n+}. The resulting Tb^{4+} ion that is formed attracts the nearest negative oxygen ions more efficiently than Tb^{3+}. As a consequence, the electron-lattice relaxation (LR) diminishes the energy of CT (or ITE) states. From the knowledge of the CT energy and LR, it is possible to locate the 4f levels of Tb^{3+} relative to the host fundamental band[43]. As pointed out in the Introduction, the host fundamental excitation (HFE) is at 37735 cm^{-1}. On the basis of the model proposed in Ref. 43, the bottom of the conduction band (i. e. the energy of the delocalized electron in $CaWO_4$) can be estimated at 1.08×HFE= 40754 cm^{-1} (5.05 eV) from the top of the valence band and defines the width of the host bandgap at ambient pressure, Eg_0. The binding energy of the electron after (Tb^{3+}-M^{n+}) CT is smaller than its binding energy after HFE. In Ref. 23, it was assumed at 1.04 times the HFE (≈ $Eg_0/1.04$) above the valence band. From this ground, the energy of the $^7F_6$ ground state of Tb^{3+}at ambient pressure can be calculated using the expression:

$$E(^7F_6, cm^{-1})_0 = \frac{Eg_0}{1.04} - (Tb^{3+} - M^{n+}, cm^{-1})_0 \qquad (4)$$

where Eg_0 is expressed in cm^{-1}. Equations (3) and (4) can be conveniently modified in order to take into account the evolution of the CT energy upon application of pressure and then predict the evolution of the whole energy level scheme of $CaWO_4$:Tb^{3+}. For this, a description of the pressure-dependence of the crystal structure and electronic properties (*viz.* the bandgap) of the $CaWO_4$ lattice is required. Using the structural data of the fergusonite phase determined at a pressure of 11.2 GPa (112 kbar)[36], the structural description of the scheelite phase at ambient pressure[44] and the pressure dependence of the lattice parameters (reported in Ref. 36) as input data, we have calculated the pressure-dependence of the average $Ca^{2+}(Tb^{3+})$-O^{2-} and of the shortest $Ca^{2+}(Tb^{3+})$-$W^{6+}$and WO_4^{2-}-WO_4^{2-}interatomic distances in the material. The results are shown in Fig. 6, and the rates of shortening have been determined and reported in Table 1 for all distances.

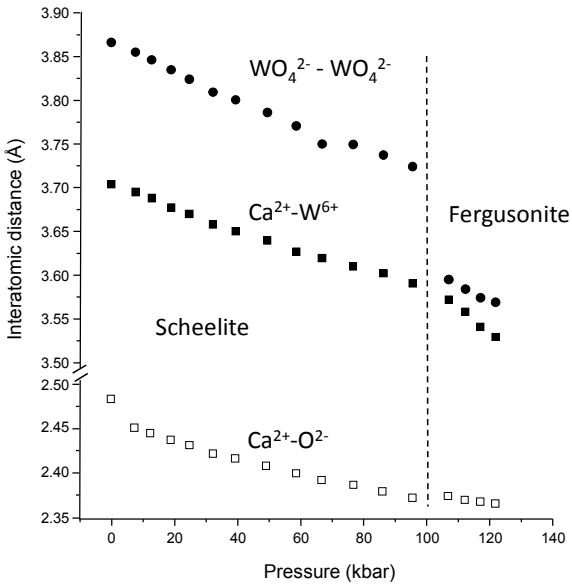

Fig. 6 Pressure dependence of relevant interatomic distances in $CaWO_4$

We point out the abrupt shrinkage of the W-W distance across the phase transition (from 3.725Å at 95.4 kbar to 3.597Å at 106.8 kbar). The effect of pressure on the electronic structure of $CaWO_4$ has been investigated in Ref. 45. It was found that the bandgap decreased at a rate of -2.1 meV/Gpa (1.7 cm^{-1}/kbar) in the scheelite phase, and much more rapidly, i. e. at a rate of -73 meV/Gpa (58.8 cm^{-1}/kbar), in the fergusonite phase. From Eqs (3) and (4), we locate the $^7F_6$ ground state of Tb^{3+} in $CaWO_4$ at ambient pressure at ≈ 7300 cm^{-1} (0.9 eV) above the top of the valence band, in correspondence with the difference 40754/1.04 - 31880. Obviously, the relevancy of the values depends on the initial choice of the bandgap value. Taking a bandgap of 5.2 eV, as done for instance in Ref. 18, or at 5.4 eV as done in Ref. 43 would shift the whole diagram to higher energies with respect to the top of the valence band. Upon application of pressure, we expect an upward shift of the 4f levels due to the shrinkage of the interatomic distances[46].This effect is concomitant with the pressure downshift of the scheelite bandgap that follows $Eg_p^S = Eg_0^S - 1.7P$, with P in kbar[45].The upper script S in this equation stands for the scheelite polymorph. We will estimate the pressure-induced downshift of the (Tb^{3+}-W^{6+}) CT state using:

$$(Tb^{3+} - W^{6+}, cm^{-1})_p^S = 58800 - 49800\,\frac{\chi_{opt}(W^{6+})}{d_p^S(Tb^{3+} - W^{6+})} \qquad (5)$$

where P is the pressure in kbar and $d_p^S(Tb^{3+} - W^{6+})$ is the shortest (pressure-dependent) distance separating the cations in the scheelite polymorph. This distance, for any value of P in the range [0 - 100 kbar], can be calculated as:

Table 1 Pressure shifts of some interatomic distances in $CaWO_4$.

Interatomic distance (Å)	Pressure shift in scheelite (10^{-3} Å/kbar)	Pressure shift in fergusonite (10^{-3} Å/kbar)
$Ca^{2+}(Tb^{3+})$-O^{2-}	-1.2	-0.7
$Ca^{2+}(Tb^{3+})$-W^{6+}	-1.2	-2.8
WO_4^{2-}-WO_4^{2-}	-1.8	-1.5

$$d_p^S(Tb^{3+}-W^{6+}) = d_0^S(Tb^{3+}-W^{6+}) - 1.210^{-3}P \quad (6)$$

The pressure dependence of the energy of the (Tb^{3+}-W^{6+}) CT state is presented in Fig. 7. The energy of the Tb^{3+} ground state can then be estimated from:

$$E(^7F_6, cm^{-1})_p^S = (Eg_0^S/1.04) - (Tb^{3+}-M^{n+}, cm^{-1})_p^S \quad (7)$$

with pressures expressed in kbar. Using the values given in [18], the energy of the excited $^5D_4$ and $^5D_3$ levels are obtained as:

$$E(^5D_4, cm^{-1})_p^S = E(^7F_6, cm^{-1})_p^S + 20520 \quad (8)$$

and

$$E(^5D_3, cm^{-1})_p^S = E(^7F_6, cm^{-1})_p^S + 26227 \quad (9)$$

The results are reproduced in Fig. 8 taking Eg_0^S = 40754 cm^{-1} and $d_0^S(Tb^{3+}-W^{6+})$ = 3.706 Å as input data. For the fergusonite polymorph, we have $Eg_p^F = Eg_0^F - 58.8P$ with Eg_0^F = 5.57 eV (44920 cm^{-1})[45]. The upper script F stands now for the fergusonite form, i. e. for P > 100 kbar. From Ref. 36, we have $d_{112}^F(Tb^{3+}-W^{6+})$ = 3.56 Å. Taking this value and the rates given in Table 1, we can obtain the Tb^{3+}-W^{6+} distances for pressures larger than 100 kbar using:

$$d_p^F(Tb^{3+}-W^{6+}) = d_{112}^F(Tb^{3+}-W^{6+}) - 2.810^{-3}(P-112) \quad (10)$$

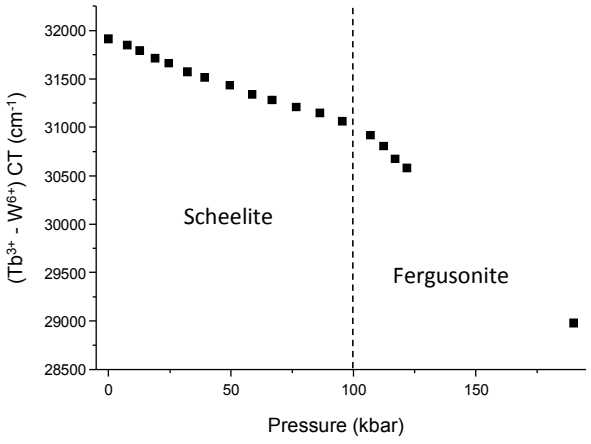

Fig. 7 Pressure dependence of the (Tb^{3+}-W^{6+}) CT energy in CaWO4:Tb^{3+}

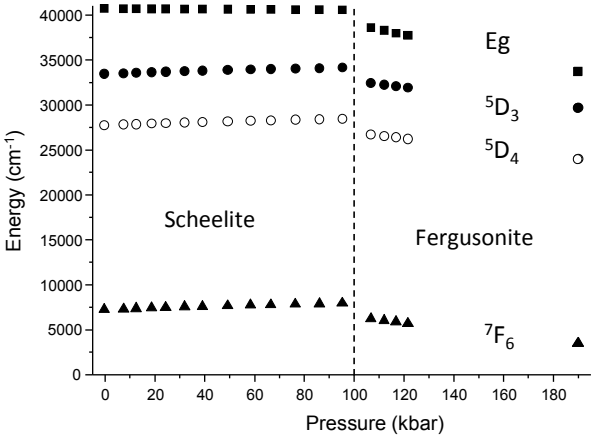

Fig. 8 Energy level scheme of $CaWO_4$:Tb^{3+} under pressure. Only the relevant levels are represented. The data are extrapolated to 190 kbar. The top of the valence band is fixed arbitrarily to energy 0.

This allows determining the (Tb^{3+}-W^{6+}) CT energy using an equation similar to Eq. (5). The energy of the $^7F_6$, $^5D_4$ and $^5D_3$ states of Tb^{3+} is then obtained by using equations similar to (7) - (9), but including the fergusonite parameters. The corresponding results are included in Fig. 8. This figure gives therefore the evolution of the energy level structure of $CaWO_4$:Tb^{3+} under hydrostatic pressure and particularly across the scheelite-to-fergusonite phase transition.As previously mentioned, the quenching at room temperature of the $^5D_3$ and $^5D_4$ states occurs at pressures of 70 and 190 kbar, respectively.

This quenching is caused by the pressure-induced downshift of the CT state in conjunction with the pressure-dependent lattice relaxation (LR) experienced by this excited state. On the basis of the arguments developed in Ref. 18, complete quenching of the emitting states occurs when the energy of these states coincide with the CT reduced by LR.

On the basis of the arguments developed in Ref. 13, complete quenching of the emitting states occurs when the energy of these states coincide with the (Tb^{3+}-W^{6+}) CT reduced by LR_P. We easily obtain the LR_P values for P = 70 and 190 kbar following:

$$LR_{70} = (Tb^{3+}-W^{6+}, cm^{-1})_{70}^S - 26227 = 5029 \ \ cm^{-1} \quad (11)$$

and

$$LR_{190} = (Tb^{3+}-W^{6+}, cm^{-1})_{190}^F - 20250 = 8730 \ \ cm^{-1} \quad (12)$$

The difference of 3700 cm^{-1} between these values compares well with the 3200 cm^{-1} downshift of CT reported in Ref. 18. It can be accounted for by an increase of the force constant of the (Tb^{3+}-W^{6+}) CT state by the action of pressure[38], especially across the scheelite – to – fergusonite phase transition. This is depicted schematically in the configuration diagrams of Fig. 9. It is worth noting here that such a modification of the CT states with pressure is consistent with the blue shift experienced by the WO_4^{2-} CT emission across the scheelite – to – fergusonite phase transition (see Fig. 2).

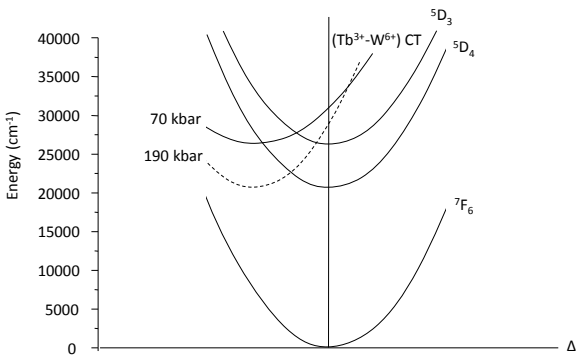

Fig. 9 Schematic one coordinate configuration diagram of $CaWO_4$:Tb^{3+} under pressure. Only the relevant levels are presented.

4. Conclusions

It is shown that the emission of Tb^{3+} is quenched at room temperature in $CaWO_4$ under the application of high pressure. This quenching is caused by a pressure-induced downshift of the charge transfer (or impurity trapped exciton) state that is formed between Tb^{3+} and nearby W^{6+} cations. This effect is a consequence of the shrinkage of the interatomic distances in the material. A model is introduced to calculate the (Tb^{3+}-W^{6+}) CT energy under pressure. Combined with the pressure dependence of the energy bandgap in $CaWO_4$, the model allows locating the 4f levels of Tb^{3+} relative to the fundamental host lattice for any pressure and is used to determine the lattice relaxation energy.

Acknowledgements

The contribution of S. M. was supported by the grant PMN 538-5200-B516-14.

References

1 F. A. Kröger, *Some aspects of the luminescence of solids*, Elsevier, Amsterdam, 1948
2. G. B. Beard, W. H. Kelly, and M. L. Mallory, J. Appl. Phys. 1962, **33**, 144
3. R. Grasser, A. Scharmann, K.-R. Strack, J. Lumin. 1982, **27**, 263
4. G. Blasse, J. Lumin. 1997, **72-74,** 129
5. V. B. Mikhailik, H. Kraus, G. Miller, M. S. Mykhaylyk, D. Wahl, J. Appl. Phys. 2005, **97**, 083523
6. V. B. Mikhailik, H. Kraus, and D. Wahl, M. Itoh and M. Koike, I. K. Bailiff, Phys. Rev. B, 2004, 69, 205110
7. F. Kang, M. Peng, Dalton Trans., 2014, **43**, 277
8. F. Kang,Y. Hu, L. Chen, X. Wang, H. Wu, Z. Mu, J. Lumin. 2013, **135**, 113
9. J. A. Groenink, G. Blasse, J. Solid State Chem. 1980, **32**, 9
10. M. J. Treadaway, R. C. Powell, J. Chem. Phys. 1974, **61**, 4003
11. F. Liang, Y. Hu, L. Chen, X. Wang, Appl. Physica A - Mater. Sci. Process. 2014, **115**, 859
12. J. Liao, B. Qiu, H. Wen, J. Chen, W. You, L. Liu, J. Alloys Compd, 2009, **487**, 758
13. X. Cheng, C. Yuan, L. Su, Y. Wang, X. Zhu, Opt. Mater. 2014, **37**, 214
14. S. Mahlik, M. Behrendt, M. Grinberg, E. Cavalli, M. Bettinelli, Opt. Mater.2012, **34**, 2012
15. E. Cavalli, P. Boutinaud, R. Mahiou, M. Bettinelli, P. Dorenbos, Inorg. Chem. 2010, **49**, 4916
16. E. G. Reut, A. I. Ryskin, Phys. Stat. Sol. (a) 1973, **17**, 47
17. M. Grinberg, S. Mahlik, J. Noncryst. Solids. 2008, **35**4, 4163
18. S. Mahlik, E. Cavalli, M. Bettinelli, M. Grinberg, Rad. Measur.2013, **56**, 1
19. S. Mahlik, M. Grinberg, E. Cavalli, M. Bettinelli, P. Boutinaud, J. Phys.: Condens. Matter 2009, **21**, 105401
20. S. Mahlik, M. Grinberg, A. A. Kaminskii, M. Bettinelli, P. Boutinaud, J. Lumin. 2009, **129**, 1219
21. S. Mahlik, M. Malinowski, M. Grinberg, Opt. Mater. 2011, **33**, 1525
22. A. Lazarowska, S. Mahlik, M. Grinberg, M. Malinowski, Photonic Letters of Poland, 2011, **3**(2), 67-69
23. S. Mahlik, M. Malinowski, M. Grinberg, Opt. Mater. 2011, **34**, 164
24. S Mahlik, M Grinberg, E Cavalli and M Bettinelli, J. Phys.: Condens. Matter., 2012, **24**, 215402
25. S. Mahlik, A. Lazarowska, B. Grobelna, M. Grinberg, J. Phys. Cond. Matter 2012, **24**, 485501
26. M. Grinberg, S. Mahlik, Crystallography Reports 2013, **58**, 147
27. S. Mahlik, M. Behrendt, M. Grinberg, E. Cavalli, M. Bettinelli, J. Phys.: Condens. Matter 2013, **25**, 105502
28. S. Mahlik, A. Lazarowska, A. Speghini, M. Bettinelli, M. Grinberg, J. Lumin. , 2014, **152**, 62
29. P. Boutinaud, R. Mahiou, E. Cavalli, M. Bettinelli J. Appl. Phys., 2004, **96**, 4923
30. P. Boutinaud, R. Mahiou, E. Cavalli, M. Bettinelli Chem. Phys. Lett., 2006, **418**, 185
31. P. Boutinaud, R. Mahiou, E. Cavalli, M. Bettinelli, J. Lumin. 2007, **122/123**, 430
32. P. Boutinaud, E. Pinel, M. Dubois, A. P. Vink, R. Mahiou, J. Lumin. 2005, **111**, 69
33. P. Boutinaud, E. Pinel, M. Oubaha, R. Mahiou, E. Cavalli M. Bettinelli, Opt. Mater. 2006, **28**, 9
34. P. Boutinaud, E. Cavalli, M. Bettinelli, J. Phys.: Condens. Matter 2007, **19**, 386230
35. P. Boutinaud, M. Bettinelli, F. Diaz,Opt. Mater.2010, **32**, 1659
36. A. Grzechnik, W. A. Crichton, M. Hanfland, S. van Smaalen, J. Phys.: Condens. Matter 2003, **15**, 7261
37. D. Errandonea, J. Pellicer-Porres, F. J. Manjón, A. Segura, Ch. Ferrer-Roca, R. S. Kumar, O. Tschauner, P. Rodríguez-Hernández, J. López-Solano, S. Radescu, A. Mujica, A. Muñoz, G. Aquilanti, Phys. Rev. B 2005, **72**, 174106
38. C. E. Tyner, H. G. Dickramer, J. Chem. Phys. 1977, **67**, 4103

39. A. A. Kubicki, P. Bojarski, M. Grinberg, M. Sadownik, B. Kuklinski, Opt. Commun. 2006, **269**, 275
40. L. Merrill, W.A. Bassett, Rev. Sci. Instrum. 1974, **45**, 290
41. R. C. Powell, G. Blasse, Struct. Bonding 1980, **42**, 43
42. C.K. Jørgensen, Prog. Inorg. Chem. 1970, **12**, 101
43. P. Dorenbos, A. H. Krumpel, E. van der Kolk, P. Boutinaud, M. Bettinelli, E. Cavalli, Opt. Mater. 2010, **32**, 1681
44. A. Zalkin, D. H. Templeton, J. Chem. Phys. 1964, **40**, 501
45. R. Lacomba-Perales, D. Errandonea, A. Segura, J. Ruiz-Fuertes, P. Rodriguez-Hernandez, S. Radescu, J. Lopez-Solano, A. Mujica, A. Munoz, J. Appl. Phys. 2011, **110**, 043703
46. P. Dorenbos, Phys. Rev. B 2012, **85**, 165107